Supporting Information

Real-Time Monitoring of the Aggregation of Alzheimer's Amyloid-β by ^{1}H Magic Angle Spinning NMR Spectroscopy

Jian Wang,[†a,b] *Tomoya Yamamoto,*[†a,b] *Jia Bai,* [a,b] *Sarah J. Cox,* [b] *Kyle J. Korshavn,*[a,b] *Martine Monnette*[c] *and Ayyalusamy Ramamoorthy*[*a,b]

[a]Biophysics Program and [b]Department of Chemistry, The University of Michigan, Ann Arbor, MI 48109-1055, USA.

[c]Bruker Canada Ltd, 2800 High Point Drive, Milton, Ontario, Canada L9T 5G5

Experimental methods

Materials and Reagents: $A\beta_{1-40}$ was purchased from BioBasic (Markham, ON, Canada, >95% purity). EGCG, D_2O (99.9% atom D), NaH_2PO_4 and Na_2HPO_4 were purchased from Sigma Aldrich (St. Louis, MO, U.S.A).

Protein preparation: A 0.1 mg aliquot of $A\beta_{40}$ which had been previously monomerized and lyophilized into a powder was dissolved in 100 µL of buffer (20 mM PO_4, pH 7.4 in 100% D_2O). The peptide was vortexed briefly and bath sonicated for 60 seconds to ensure the dissolution and complete monomerization. The concentration of the peptide solution was then evaluated by UV-Vis (extinction coefficient 1450). This concentrated stock was subsequently diluted using buffer to the desired peptide concentration. All preparations were done on ice to minimize the initial aggregation of the peptide.

NMR spectroscopy: All NMR experiments were performed at 298 K on a Bruker 500 MHz solution/solid-state NMR spectrometer using a comprehensive multiphase (CMP) NMR probe. 50 µL freshly prepared $A\beta_{40}$ solution was packed in a 4 mm zirconia rotor (purchased from Bruker) which was washed with hexane. KEL-F top insert was used for avoiding the leakage of sample from the rotor under spinning. 1D ^1H NMR spectra were obtained using the Carr-Purcell-Meiboom-Gill pulse sequence with 1024 scans for 50 µM and 150 µM, 5000 scans for 25 µM, 10000 scans for 15 µM of $A\beta_{40}$ samples and 10000 scans for 50 µM of $A\beta_{40}$ with 50 µM of EGCG

samples. The spectral width was 8,012.82 Hz and water pre-saturation was used to suppress the residual HDO peak from the sample.

Transmission electron microscopy: Samples used in TEM analysis were taken directly from the NMR rotor after spinning for dozens of hours. Glow-discharged grids (Formar/carbon 300 mesh, Electron Microscopy Sciences, Hatfield, PA) were treated with samples (7 μl) for 1 min at room temperature. Excess buffer was removed via blotting and then washed three times with double-distilled H_2O. Each grid was then incubated with uranyl acetate staining solution (1% (w/v) in double-distilled H2O) for 1 min, and excess stain was blotted away. Images from each sample were taken on a JEOL 1400-plus TEM (80 kV) at X 10,000 magnification.

H_2N - Asp^{1} - Ala^{2} - Glu^{3} - Phe^{4} - Arg^{5} - His^{6} - Asp^{7} - Ser^{8} - Gly^{9} - Tyr^{10} -
Glu^{11} - Val^{12} - His^{13} - His^{14} - Gln^{15} - Lys^{16} - Leu^{17} - Val^{18} - Phe^{19} - Phe^{20} -
Ala^{21} - Glu^{22} - Asp^{23} - Val^{24} - Gly^{25} - Ser^{26} - Asn^{27} - Lys^{28} - Gly^{29} - Ala^{30} -
Ile^{31} - Ile^{32} - Gly^{33} - Leu^{34} - Met^{35} - Val^{36} - Gly^{37} - Gly^{38} - Val^{39} - Val^{40} - COOH

Conversion of the intrinsically disordered protein a-synuclein (a-syn) into amyloid aggregates is a k ey process in

ParkinsonÏs disease. T he sequence region 35–59 contains b-strand segments b1 a nd b2 o f a-syn amyloid fibril models and most disease-related mutations. b1 a nd

b2 f requently engage in transient interactions in monomeric a-syn. The consequences of b1–
b2 c ontacts are evaluated by disulfide engineering,

biophysical techniques, a nd cell viability assays. T he double-cysteine mutant a-synCC, w ith a d isulfide linking b1 a nd b2, is aggregation-incompetent and

inhibits aggregation and toxicity of wild-type a-syn. We show that a-syn delays t he aggregation of amyloid-b peptide and islet amyloid

polypeptide involved in AlzheimerÏs disease and type 2 d iabetes, a n e f fect enhanced in the a-synCC mutant. Tertiary interactions in the b1–b2 r egion

of a-syn interfere with the nucleation of amyloid formation, suggesting promotion of such interactions as a p otential therapeutic approach.

Conversion of the intrinsically disordered protein a-synuclein (a-syn) into amyloid aggregates is a k ey process in ParkinsonÏs disease. T he

sequence region 35–59 contains b-strand segments b1 a nd b2 o f a-syn amyloid fibril models and most disease-related mutations. b1 a nd b2 f requently engage in

transient interactions in monomeric a-syn. The consequences of b1–b2 c ontacts are evaluated by disulfide engineering, biophysical techniques, a nd

cell viability assays. T he double-cysteine mutant a-synCC, w ith a d isulfide linking b1 a nd b2, is aggregation-incompetent and inhibits

aggregation and toxicity of wild-type a-syn. We show that a-syn delays t he aggregation of amyloid-b peptide and islet amyloid polypeptide involved in

Alzheimer Ïs disease and type 2 d iabetes, a n e f fect enhanced in the a-synCC mutant. Tertiary interactions in the b1–b2 r egion of a-syn interfere with the nucleation

of amyloid formation, suggesting promotion of such interactions as a p otential therapeutic approach. Conversion of the intrinsically

disordered protein a-synuclein (a-syn) into amyloid aggregates is a k ey process in ParkinsonÏs disease. T he sequence region 35–59 contains b-

strand segments b1 a nd b2 o f a-syn amyloid fibril models and most disease-related mutations. b1 a nd b2 f requently engage in transient interactions in

monomeric a-syn. The consequences of b1–b2 c ontacts are evaluated by disulfide engineering, biophysical techniques, a nd cell viability

assays. T he double-cysteine mutant a-synCC, w ith a d isulfide linking b1 a nd b2, is aggregation-incompetent and inhibits aggregation and toxicity

of wild-type a-syn. We show that a-syn delays t he aggregation of amyloid-b peptide and islet amyloid polypeptide involved in AlzheimerÏs disease and type

2 d iabetes, a n e f fect enhanced in the a-synCC mutant. Tertiary interactions in the b1–b2 r egion of a-syn interfere with the nucleation of amyloid formation,

suggesting promotion of such interactions as a p otential therapeutic approach. Conversion of the intrinsically disordered protein a-

synuclein (a-syn) into amyloid aggregates is a k ey process in ParkinsonÏs disease. T he sequence region 35–59 contains b-strand segments b1 a nd b2 o f a-

syn amyloid fibril models and most disease-related mutations. b1 a nd b2 f requently engage in transient interactions in monomeric a-syn. The consequences

of b1–
b2 c ontacts are evaluated by disulfide engineering, biophysical techniques, a nd cell viability assays. T he double-

cysteine mutant a-synCC, w ith a d isulfide linking b1 a nd b2, is aggregation-incompetent and inhibits aggregation and toxicity of wild-type a-syn. We show that a-

syn delays t he aggregation of amyloid-b peptide and islet amyloid polypeptide involved in AlzheimerÏs disease and type 2 d iabetes, a n e f fect enhanced in

the a-synCC mutant. Tertiary interactions in the b1–b2 r egion of a-syn interfere with the nucleation of amyloid formation, suggesting promotion of such

interactions as a p otential therapeutic approach. Conversion of the intrinsically disordered protein a-synuclein (a-syn) into amyloid

aggregates is a key process in ParkinsonÏs disease. The sequence region 35–59 contains b-strand segments b1 and b2 of a-syn amyloid fibril models and

most disease-related mutations. b1 a nd b2 f requently engage in transient interactions in monomeric a-syn. The consequences of b1–b2 c ontacts are

evaluated by disulfide engineering, biophysical techniques, a nd cell viability assays. T he double-cysteine mutant a-synCC, w ith

a d isulfide linking b1 a nd b2, is aggregation-incompetent and inhibits aggregation and toxicity of wild-type a-syn. We show that a-syn delays t he aggregation

of amyloid-b peptide and islet amyloid polypeptide involved in AlzheimerÏs disease and type 2 d iabetes, a n e f fect enhanced in the a-synCC mutant. Tertiary

interactions in the b1–b2 r egion of a-syn interfere with the nucleation of amyloid formation, suggesting promotion of such interactions as a p otential

therapeutic approach. Conversion of the intrinsically disordered protein a-synuclein (a-syn) into amyloid aggregates is a k ey process in

ParkinsonÏs disease. T he sequence region 35–59 contains b-strand segments b1 a nd b2 o f a-syn amyloid fibril models and most disease-related mutations. b1 a nd

b2 f requently engage in transient interactions in monomeric a-syn. The consequences of b1–
b2 c ontacts are evaluated by disulfide engineering,

biophysical techniques, a nd cell viability assays. T he double-cysteine mutant a-synCC, w ith a d isulfide linking b1 a nd b2, is aggregation-incompetent and

inhibits aggregation and toxicity of wild-type a-syn. We show that a-syn delays t he aggregation of amyloid-b peptide and islet amyloid

polypeptide involved in AlzheimerÏs disease and type 2 d iabetes, a n e f fect enhanced in the a-synCC mutant. Tertiary interactions in the b1–b2 r egion

of a-syn interfere with the nucleation of amyloid formation, suggesting promotion of such interactions as a p otential therapeutic approach.

Conversion of the intrinsically disordered protein a-synuclein (a-syn) into amyloid aggregates is a k ey process in ParkinsonÏs disease. T he

sequence region 35–59 contains b-strand segments b1 a nd b2 o f a-syn amyloid fibril models and most disease-related mutations. b1 a nd b2 f requently engage in

transient interactions in monomeric a-syn. The consequences of b1–b2 c ontacts are evaluated by disulfide engineering, biophysical techniques, a nd

cell viability assays. T he double-cysteine mutant a-synCC, w ith a d isulfide linking b1 a nd b2, is aggregation-incompetent and inhibits

aggregation and toxicity of wild-type a-syn. We show that a-syn delays t he aggregation of amyloid-b peptide and islet amyloid polypeptide involved in

AlzheimerÏs disease and type 2 d iabetes, a n e f fect enhanced in the a-synCC mutant. Tertiary interactions in the b1–b2 r egion of a-syn interfere with the nucleation

of amyloid formation, suggesting promotion of such interactions as a p otential therapeutic approach.

Abstract:

Conversion of the intrinsically

disordered protein a-synuclein (a-syn) into amyloid aggregates is a k ey process in ParkinsonÏs d

Abstract: Conversion of the intrinsically

disordered protein a-synuclein (a-syn) into amyloid aggregates is a k ey process in ParkinsonÏs d

Abstract:

Conversion of the intrinsically

disordered protein a-synuclein (a-syn) into amyloid aggregates is a k ey process in ParkinsonÏs d

Abstract:

Conversion of the intrinsically

disordered protein a-synuclein (a-syn) into amyloid aggregates is a k ey process in ParkinsonÏs d

Abstract:

Conversion of the intrinsically

disordered protein a-synuclein (a-syn) into amyloid aggregates is a k ey process in ParkinsonÏs d

Figure S1. The amino acid sequence of amyloid beta (Aβ)–1-40 peptide. Red-colored residues contain aromatic side chains.

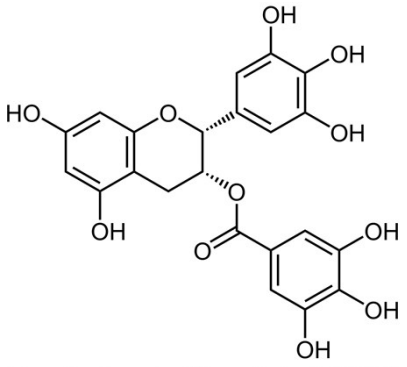

(-)-epigallocatechin gallate (EGCG)

Figure S2. Chemical structure of EGCG extracted from green-tea.

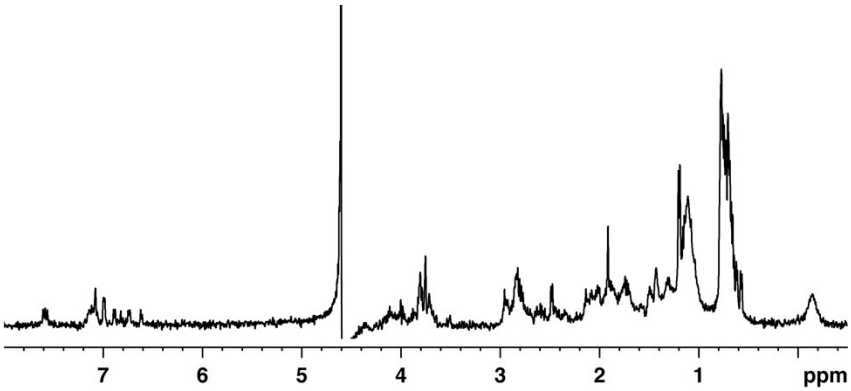

Figure S3. 1D ^{1}H NMR spectrum of freshly prepared 50 μM $A\beta_{1\text{-}40}$ under 5 kHz MAS and 298 K.

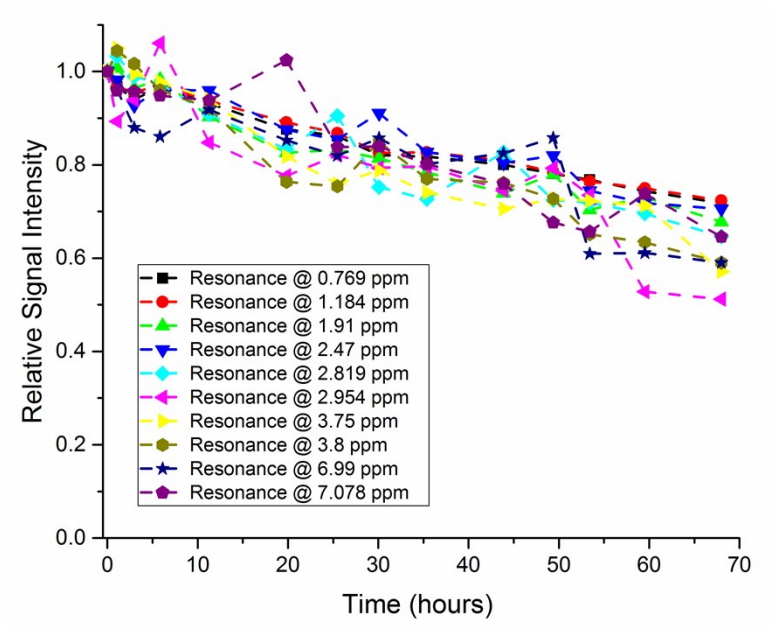

Figure S4. Depletion of $A\beta_{1\text{-}40}$ monomers under MAS. Intensity of proton resonances at different sites measured as a function of aggregation time oft he peptide under 5 kHz MAS and 298 K.

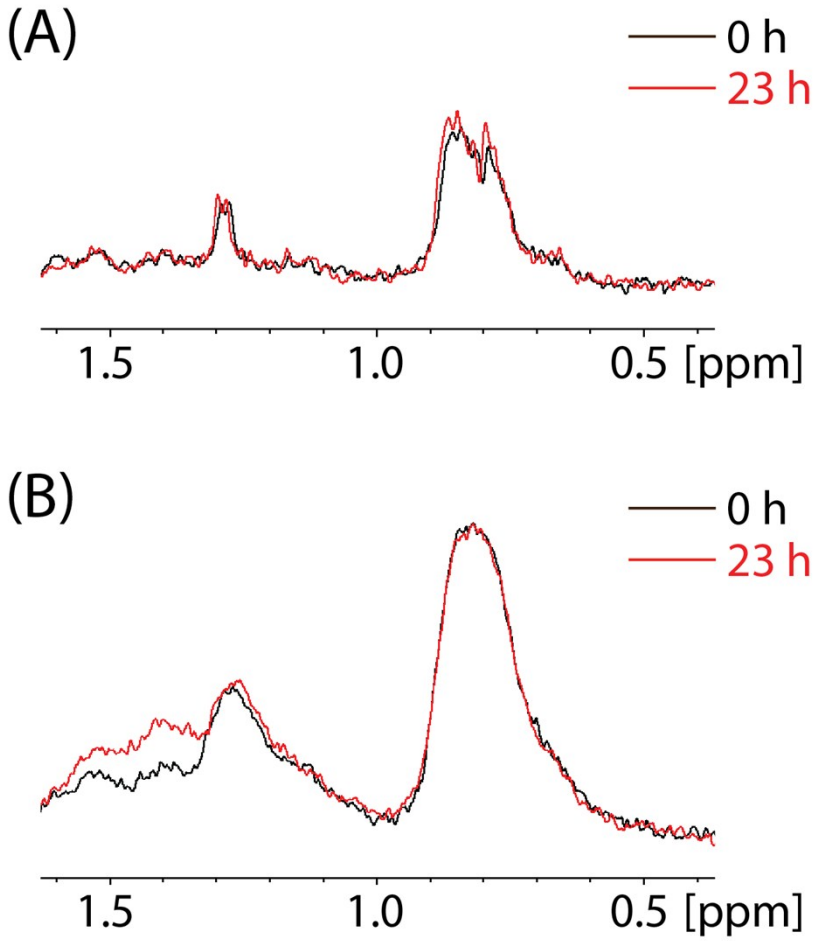

Figure S5. 1D ^{1}H NMR spectra of 50 µM A$\beta_{1\text{-}40}$ under quiescent condition. ^{1}H NMR spectra of 50 µM of Aβ_{40} solution in (A) 5 mm Shigemi NMR tube and (B) 4 mm ZrO_2 MAS rotor placed inside a 5 mm solution NMR tube. No signal decay was observed after 23 h, which indicates that the signal decay under MAS results from the acceleration due to the mechanical rotation of the sample under MAS.

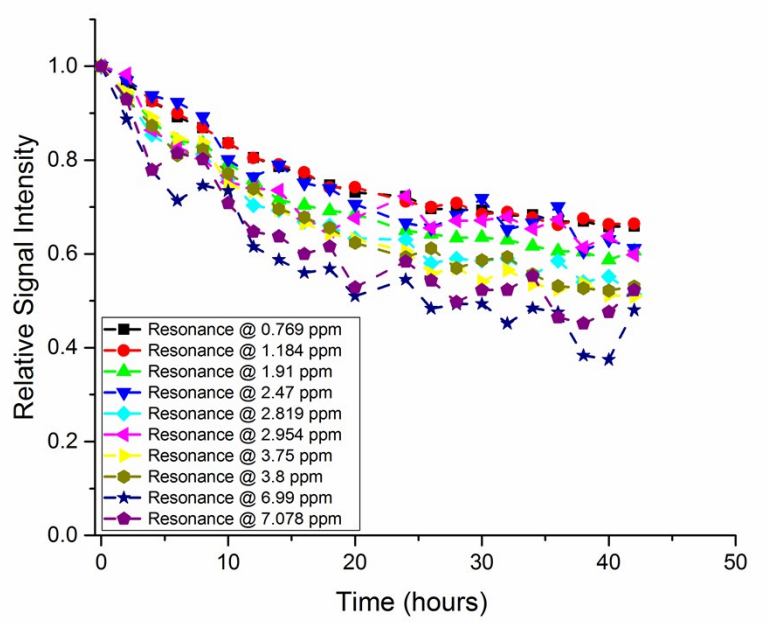

Figure S6. Depletion of $A\beta_{1\text{-}40}$ monomers under MAS in presence of EGCG. Intensities of proton resonances at different sites measured as a function of time under 5 kHz MAS and 298 K.

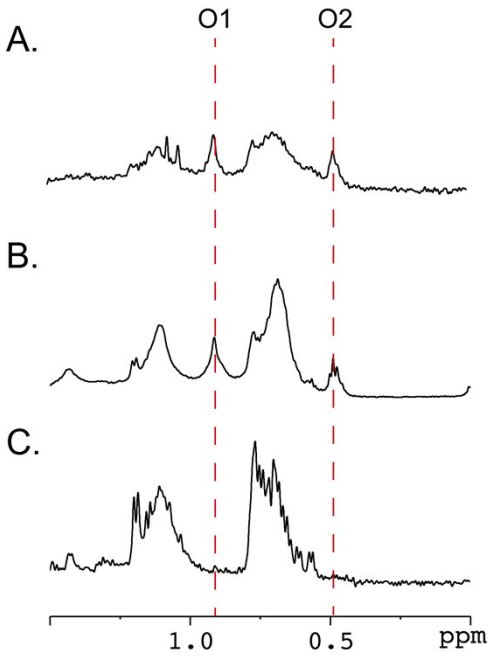

Figure S7. Low-frequency region of 1D ^{1}H NMR spectra of $A\beta_{1\text{-}40}$ after spinning under 5 kHz MAS. (A) ^{1}H NMR spectrum of 5 μM $A\beta_{1\text{-}40}$ without EGCG after spinning for 90 hours. (B) ^{1}H NMR spectrum of 50 μM $A\beta_{40}$ with EGCG after spinning for 42 hours. (C) ^{1}H NMR spectrum of 50 μM $A\beta_{1\text{-}40}$ without EGCG after spinning for 68 hours.

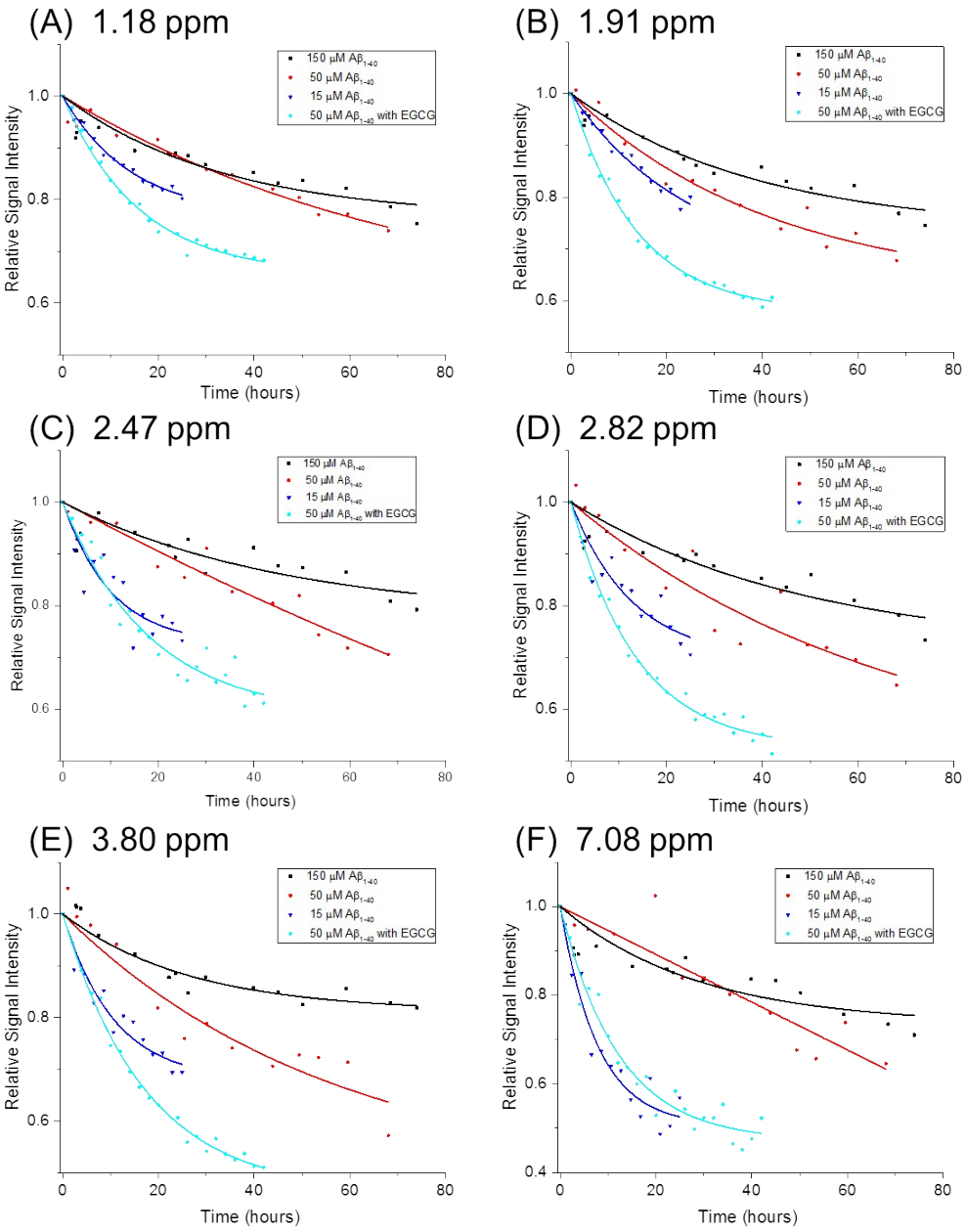

Figure S8. Concentration-dependent depletion of Aβ$_{1-40}$ monomers. ^{1}H NMR signal decay measured for different resonance under 5 kHz MAS for the indicated peptide concentration.

Table S1. Parameters obtained by fitting the monomer decay curves. The decay curves measured from NMR experiments were fitted using the equation y=(1-A)*exp(-b*x)+A. [a]Curve did not fit well with experimental data under these conditions.

		150 μM	50 μM	15 μM	50 μM + EGCG
1.18 ppm	A	0.76	0.57	0.78	0.66
	b	0.030	0.028	0.030	0.063
1.91 ppm	A	0.74	0.62	0.66	0.58
	b	0.026	0.024	0.040	0.072
2.47 ppm	A	0.78	-0.21[a]	0.73	0.59
	b	0.022	0.004[a]	0.099	0.055
2.82 ppm	A	0.71	0.48	0.70	0.52
	b	0.020	0.015	0.078	0.073
3.80 ppm	A	0.81	0.48	0.68	0.46
	b	0.038	0.018	0.094	0.058
7.08 ppm	A	0.73	-1.66×10^{4} [a]	0.51	0.47
	b	0.035	3.244×10^{-7} [a]	0.128	0.082

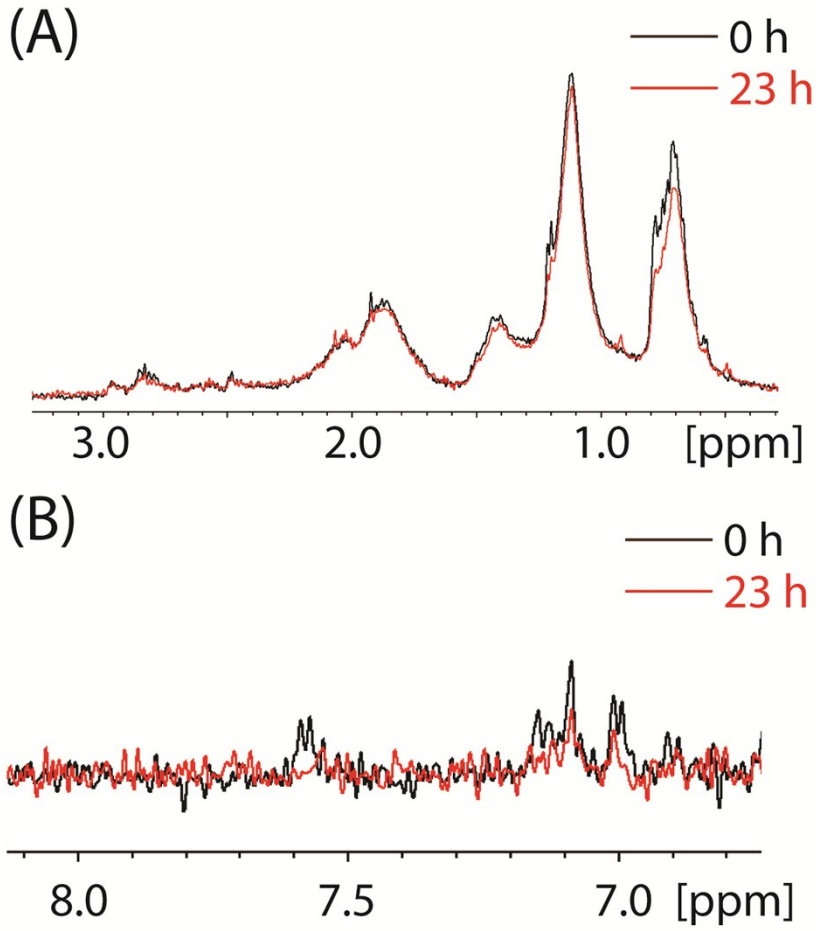

Figure S9. Proton NMR spectra of 5:3 $A\beta_{1-40}$:EGCG solution under 5 kHz MAS. ^{1}H NMR spectra acquired under 5 kHz MAS for a solution of 25 µM of $A\beta_{1-40}$ and 15 µM of EGCG at room temperature at 0 and after 23 hours are compared. Signal decay observed after 23 hours is in agreement with the results shown in the main text. Observed signal decays resulted in an intensity reduction of 30% for aliphatic protons (0.78 ppm) and 47% for aromatic protons (7.00 ppm), which are similar to that observed for 50 µM of $A\beta_{1-40}$ and 50 µM of EGCG solution (28% and 46% at t=24 hours, respectively) as shown in Figures 2 and 4.